Molecular Biology of the Cell
Vol. 20, 4205–4215, October 1, 2009

mTrs130 Is a Component of a Mammalian TRAPPII Complex, a Rab1 GEF That Binds to COPI-coated Vesicles

Akinori Yamasaki,*† Shekar Menon,*† Sidney Yu,*‡ Jemima Barrowman,*§ Timo Meerloo,‖ Viola Oorschot,¶ Judith Klumperman,¶ Ayano Satoh,#@ and Susan Ferro-Novick*†

*Department of Cell Biology, Howard Hughes Medical Institute, Yale University School of Medicine, New Haven, CT 06519; ‖Department of Cellular and Molecular Medicine, University of California at San Diego, La Jolla, CA 92093-0651; #Department of Cell Biology, Yale University School of Medicine, New Haven, CT 06520; and ¶Cell Microscopy Center, Department of Cell Biology, University Medical Center Utrecht, Utrecht, The Netherlands

Submitted May 13, 2009; Revised July 22, 2009; Accepted July 24, 2009
Monitoring Editor: Akihiko Nakano

The GTPase Rab1 regulates endoplasmic reticulum-Golgi and early Golgi traffic. The guanine nucleotide exchange factor (GEF) or factors that activate Rab1 at these stages of the secretory pathway are currently unknown. Trs130p is a subunit of the yeast TRAPPII (transport protein particle II) complex, a multisubunit tethering complex that is a GEF for the Rab1 homologue Ypt1p. Here, we show that mammalian Trs130 (mTrs130) is a component of an analogous TRAPP complex in mammalian cells, and we describe for the first time the role that this complex plays in membrane traffic. mTRAPPII is enriched on COPI (Coat Protein I)-coated vesicles and buds, but not Golgi cisternae, and it specifically activates Rab1. In addition, we find that mTRAPPII binds to γ1COP, a COPI coat adaptor subunit. The depletion of mTrs130 by short hairpin RNA leads to an increase of vesicles in the vicinity of the Golgi and the accumulation of cargo in an early Golgi compartment. We propose that mTRAPPII is a Rab1 GEF that tethers COPI-coated vesicles to early Golgi membranes.

INTRODUCTION

In mammals, traffic between the endoplasmic reticulum (ER) and Golgi complex requires the sequential action of two different coat complexes, COPII (Coat Protein II) and COPI (Aridor *et al*., 1995). These coat complexes are needed for cargo selection and vesicle budding. COPII-coated vesicles bud from a specialized region of the ER, called the transitional ER (tER), and then tether and fuse with each other (homotypic tethering/fusion) to form vesicular tubular clusters (VTCs), a pre-Golgi compartment (Stephens *et al*., 2000; Xu and Hay, 2004). At this compartment, another coat complex called COPI (coat protein I) is recruited onto membranes. Although COPII vesicles only mediate traffic between the ER and VTCs, COPI vesicles have been implicated in multiple trafficking pathways. The clearest of these trafficking pathways are from the VTCs to the ER and within the Golgi complex (Bonifacino and Lippincott-Schwartz, 2003).

This article was published online ahead of print in *MBC in Press* (http://www.molbiolcell.org/cgi/doi/10.1091/mbc.E09–05–0387) on August 5, 2009.

Present addresses: † Department of Cellular and Molecular Medicine, Howard Hughes Medical Institute, University of California, San Diego, La Jolla, CA 92093-0668; ‡ School of Biomedical Sciences and Epithelial Cell Biology Research Center, The Chinese University of Hong Kong, Shatin, New Territories, Hong Kong; § Department of Cell Biology, The Johns Hopkins School of Medicine, Baltimore, Maryland, MD, 21205; @ Research Core for Interdisciplinary Sciences, Okayama University, Okayama 700-8530, Japan.

Address correspondence to: Susan Ferro-Novick (sfnovick@ucsd.edu).

The GTPase Rab1 regulates both ER-Golgi and early Golgi traffic (Plutner *et al*., 1991; Allan *et al*., 2000; Moyer *et al*., 2001). In ER-Golgi traffic, activated Rab1 is required for the recruitment of the tethering factor p115 onto COPII vesicles (Allan *et al*., 2000). Tethering is a term that has been used to describe the initial interaction of a transport vesicle with its target membrane (Pfeffer, 1999; Whyte and Munro, 2002; Cai *et al*., 2007a). Activated Rab1 also interacts with a Golgi-associated macromolecular complex to mediate vesicle tethering/fusion in early Golgi traffic. This macromolecular complex includes the tethering factors GM130 and Giantin (Davidson and Balch, 1993; Moyer *et al*., 2001; Beard *et al*., 2005). Thus, Rab1 seems to regulate ER-to-Golgi (COPII vesicle tethering) and early Golgi traffic (COPI vesicle tethering) via different effectors. The guanine nucleotide exchange factor (GEF) that activates Rab1 is currently unknown.

In the yeast *Saccharomyces cerevisiae*, several essential subunits of the transport protein particle (TRAPP) complexes are required to activate the Rab1 homologue Ypt1p (Kim *et al*., 2006; Cai *et al*., 2008); two copies of Bet3p; and one copy each of Bet5p, Trs23p, and Trs31p (Cai *et al*., 2008). These subunits are found in both the TRAPPI and TRAPPII complexes. TRAPPI is required for COPII vesicle tethering (Cai *et al*., 2007b), whereas TRAPPII acts after TRAPPI (Sacher *et al*., 2001; Cai *et al*., 2005). The TRAPPI and TRAPPII complexes share several subunits, whereas three additional subunits (Trs130p, Trs120p, and Trs65p) are unique to TRAPPII (Sacher *et al*., 2001).

Previous studies have shown that mammalian Bet3 (mBet3) is recruited to the tER where it mediates homotypic COPII vesicle tethering by binding to a subunit of the COPII

coat cargo adaptor complex (Yu *et al*., 2006; Cai *et al*., 2007b) that sorts cargo into COPII vesicles (Kuehn *et al*., 1998). This event is required for the formation of VTCs (Yu *et al*., 2006). Here, we show that mBet3 is also a component of a high-molecular-weight TRAPP complex that is a Rab1 GEF. This complex contains the TRAPPII-specific subunits mTrs130 and mTrs120. Mammalian TRAPPII (mTRAPPII) is enriched on COPI-coated Golgi vesicles and buds and not Golgi cisternae. In addition, we show that mTRAPPII binds to the COPI coat adaptor subunit, γ1COP. Consistent with a role for mTRAPPII in tethering COPI-coated vesicles, the depletion of mTrs130 leads to a block in anterograde traffic and cargo accumulates in the early Golgi. We propose that mTrs130 is a component of a mammalian Rab1 GEF that mediates a COPI-dependent early Golgi vesicle-tethering event.

MATERIALS AND METHODS

Antibodies

Monoclonal antibody (mAb) directed against GM130, and anti-Sec31A antibody was purchased from BD Biosciences (San Jose, CA). Anti-γ-adaptin antibody was purchased from Sigma-Aldrich (St. Louis, MO). Monoclonal antibodies directed against COPI (CM1A10), vesicular stomatitis virus G (VSV-G) ectodomain, and ER–Golgi intermediate compartment (ERGIC)-53 were obtained from G. Warren (Yale University, New Haven, CT) and H.-P. Hauri (University of Basel, Basel, Switzerland), respectively. Anti-mBet3 antibody was described previously (Yu *et al*., 2006). Rabbit anti-mTrs130 (TRAPPC10) antibody was raised to a maltose-binding protein (MBP) fusion protein that contained amino acids 1116-1259 (GenBank accession NP_003265). The antibody was purified by incubating serum with a nitrocellulose strip that contained the fusion protein. Anti-mTrs23 antibody was raised to an MBP fusion of full-length mouse Trs23 (GenBank accession NP_068561). The antibody was purified by incubating serum with a nitrocellulose strip that contained the fusion protein. Rabbit anti-mTrs120 (NIK and IKKβ binding protein [NIBP]) antibody was raised to an MBP fusion protein that contained amino acids 661-994 (GenBank accession NP_083916). To purify anti-mTrs120 antibody, serum was first loaded onto an Affigel column (Bio-Rad Laboratories, Hercules, CA) that was preloaded with MBP. The flow-through was collected and incubated with a nitrocellulose strip that contained the fusion protein. Bound immunoglobulin (IgG) was eluted with 0.1 M glycine, pH 2.0. Affinity-purified anti-mTrs130 and mTrs120 antibodies did not disrupt the architecture of the Golgi or membrane traffic. Thus, these antibodies do not inactivate mTrs130 or mTrs120 function. Polyclonal antibody BSTR against β′COPI was a kind gift of R. Pepperkok (EMBL, Heidelberg, Germany). Fluorescently labeled secondary antibodies were purchased from Invitrogen.

Fluorescence Microscopy

COS-7 cells were grown on 10-mm coverslips in DMEM with high glucose and supplemented with 10% fetal bovine serum (Invitrogen, Carlsbad, CA). For the brefeldin A (BFA) (Sigma-Aldrich) experiment, BFA (5 μg/ml, final concentration) was added to the growth medium, and the sample was incubated for 30 min. For the nocodazole (Sigma-Aldrich) experiments, nocodazole (10 μg/ml, final concentration) was added to the growth medium, and the sample was incubated for 60 min. At the end of the incubation, the coverslip was washed once in phosphate-buffered saline (PBS), and then the cells were fixed and permeabilized for 15 min on ice with cold methanol. The coverslip was then washed with PBS containing 0.5% bovine serum albumin (BSA) and incubated with PBS plus 5% BSA for 60 min. The cells were then incubated with primary antibody for 60 min, and washed three times with PBS plus 0.5% BSA. For each wash, the sample was soaked for 5 min in buffer. The cells were then treated with secondary antibody in the same way, and the coverslip was mounted on a slide containing Fluoremount G (Southern Biotech, Birmingham, AL). The primary antibodies used in this study were anti-mTrs130 (3 μg/ml), anti-mTrs23 (1 μg/ml), anti-GM130, anti-ERGIC-53, anti-Sec31A, anti-γ-adaptin, COPI and GalT. The secondary antibodies used to localize mTrs130 were anti-rabbit IgG conjugated to Alexa 488. Anti-mouse IgG conjugated to Alexa 594 was used to localize ERGIC-53, GM130, γ-adaptin, COPI, GalT, and Sec31A. Images were taken with an LSM 510 confocal microscope or an AxioVision fluorescence microscope using a 63× objective, and captured with a digital AxioCam MRm camera (Carl Zeiss Microimaging, Thornwood, NY). For quantitation of the VSV-G trafficking experiment described below, the area of the cell and Golgi region was defined manually, and the mean fluorescence was measured using Photoshop (Adobe Systems, San Jose, CA). To normalize the data, at least 27–49 cells were analyzed from three independent experiments.

RNA Interference and VSV-G Trafficking

Vectors that target mTrs130 mRNA were constructed using short hairpin RNA (shRNA) expression vector pSilencer 1.0-U6 (Ambion, Austin, TX). Two mTrs130 shRNA vectors were constructed, vector1-targeted nucleotide bases 826-844 (5′-GTGAAGAGCTGGAACGGAT-3′), whereas vector 2 targeted 3326-3344 (5′-GTGAAGAGCTGGAACGGAT-3′). The pSilencer 1.0-U6 vector (empty vector control), as well as vectors 1 and 2, was transfected twice into COS-7 cells by using FuGENE 6 buffer (Roche Diagnostics, Indianapolis, IN). The second transfection was done 48 h after the first transfection. The cells were harvested 48 h after the second transfection. Samples were quantitated from three independent experiments as described previously (Yu *et al*., 2006).

For the complementation experiment, COS-7 cells were transfected with pSilencer 1.0-U6 or vector 1 at 37°C. Two days later, the cells were transfected with an expression vector that expresses green fluorescent protein (GFP) or GFP-mTrs130* and then immunostained 48 h later. The vector (pEGFP-C3) that expressed GFP-mTrs130* contained three silent mutations (831 G to A, 834 C to T, and 840 C to T) in the region that encodes mTrs130.

For the VSV-G-GFP trafficking experiments, four different samples were transfected with pEGFPdKA206K-N1-VSVG tsO45 (Patterson *et al*., 2008) during the second round of transfection. All samples were incubated at 37°C for 24 h and then shifted to 42°C for 20 h. Cycloheximide was added to a final concentration of 10 μg/ml for 30 min before the cells were shifted to 32°C. Samples were incubated at 32°C for 30, 60, and 90 min.

VSV-G transport was measured as described previously (Seemann *et al*., 2000). In brief, cells were treated as described above and then fixed in 3.7% paraformaldehyde for 15 min and stained with anti-VSV-G ectodomain antibody (primary antibody) and anti-mouse IgG conjugated to cyanine 5 (secondary antibody). Total VSV-G-GFP fluorescence was quantified as described previously (Seemann *et al*., 2000). All images were captured at the same setting and exposure. Cell area (A) was defined manually. The mean (I) of the fluorescence intensity in the area was measured by Photoshop CS2. The integrated optical density (IOD) was determined by the formula IOD = AxI. Differences in expression level were corrected by determining the ratio of cell surface-to-total VSV-G IOD. This was determined for thirty cells per experiment, and the SEM was calculated from four independent experiments.

Electron Microscopy (EM) Analysis of mTrs130-depleted Cells

EM was performed as described previously (Yu *et al*., 2006). The number of vesicles accumulating in the Golgi area was defined as described in Seemann *et al*. (2000).

The area was estimated by the point hit method (Weibel and Bolender, 1979) with an 80-nm square grid. Small vesicles were defined as circular profiles with a diameter of 50–80 nm within the Golgi area. The results are expressed as the number of vesicles per square micrometer of the Golgi area. Quantification of the amount of membrane that represents Golgi cisternae was done as described previously (Yu *et al*., 2006).

Preparation of NIH3T3 Cytosol and Gel Filtration Chromatography

NIH3T3 cells were maintained in DMEM with high salt and supplemented with 10% fetal calf serum (Invitrogen). Procedures for preparing cytosol from NIH3T3 cells were described previously (Sacher *et al*., 2000). In brief, ten 15-cm plates of NIH3T3 cells at 70–80% confluence were trypsinized and washed with PBS. Cytosol was prepared by Dounce homogenization in 1 ml of lysis buffer (20 mM HEPES, pH 7.2). Then, NaCl, EDTA, and dithiothreitol (DTT) were added to a final concentration of 150, 2, and 1 mM, respectively, before protease inhibitor cocktail (as described in Waters and Blobel, 1986) was added to 1× concentration. The lysate was centrifuged at 100,000 × *g* for 1 h, and the supernatant was removed from the pellet. Approximately 2 mg of cytosol was loaded onto an FPLC Superdex-200 gel filtration column (GE Healthcare, Chalfont St. Giles, Buckinghamshire, United Kingdom), and 1-ml fractions were collected. The fractions were concentrated by trichloroacetic acid precipitation and resuspended in 120 μl of 1× SDS sample buffer. Samples (30 μl) were analyzed by SDS-polyacrylamide gel electrophoresis and Western blot analysis.

Immuno-EM

Cells were fixed by adding 4% freshly prepared formaldehyde in 0.1 M phosphate buffer, pH 7.4, to an equal volume of culture medium for 10 min, followed by postfixation in 4% formaldehyde in 0.1 M phosphate buffer, pH 7.4, without medium. Cells were stored until further processing in 1% formaldehyde at 4°C. Processing of cells for ultrathin cryosectioning and immunolabeling according to the protein A-gold method was done as described previously (Slot and Geuze, 2007). In brief, fixed cells were washed with 0.05 M glycine in PBS, scraped gently from the dish in PBS containing 1% gelatin, and pelleted in 12% gelatin in PBS. The cell pellet was solidified on ice and cut into small blocks. For cryoprotection, blocks were infiltrated overnight with 2.3 M sucrose at 4°C and then mounted on aluminum pins and frozen in liquid nitrogen. To pick up ultrathin cryosections, a 1:1 mixture of 2.3 M

sucrose and 1.8% methylcellulose was used (Liou *et al*., 1996). Affinity-purified anti-mTrs23 (1.8 mg/ml) was diluted 1:15. β′COP antibody was diluted 1:200.

Multiple grids dual-labeled for mTrs23 and β′COP were examined and quantitated by electron microscopy and grouped as follows: ER, pre-Golgi, Golgi, *trans*-Golgi network (TGN), and peripheral vesicles. For the TGN, a 400-nm area on the *trans* side of the Golgi was counted. To quantitate the number of gold particles associated with peripheral Golgi vesicles and buds, an area extending ~200 nm on either side of the Golgi was scored.

Immunoprecipitation of the Mammalian TRAPPII Complex

For the preparation of NIH3T3 lysate, cell pellets harvested from ten 15-cm plates were resuspended in 2 ml of lysis buffer (20 mM HEPES, pH 7.2, and 150 mM NaCl) containing 0.1% Triton X-100. The mixture was centrifuged in a table top centrifuge at 3000 rpm for 5 min. The supernatant was collected, and the pellet was re-extracted in the same way. After the second extraction, the pellet was resuspended in 2 ml of lysis buffer containing 0.5% Triton X-100 and extracted again. The supernatants were combined and centrifuged at 16,000 × *g* for 10 min. The resulting supernatant was incubated overnight at 4°C (with agitation) with 10 μg of purified anti-mTrs130 IgG, anti-mTrs120 (NIBP) IgG or nonspecific IgG, and 50 μl of a slurry of protein A-Sepharose beads. The next day, the beads were washed twice with lysis buffer containing 0.1% Triton X-100 and then two more times with lysis buffer. The beads were analyzed by Western blot analysis or assayed for their ability to stimulate Rab1 GEF activity. To precipitate mTRAPP from Superdex-200 column fractions, fractions 9 and 10 were combined, and 10 μg of purified anti-mTrs120 IgG, anti-mBet3 IgG, or nonspecific IgG was incubated overnight at 4°C with 50 μl of a slurry of protein A-Sepharose beads. The next day, the beads were washed and analyzed as described above.

Nucleotide Exchange Assays

Expression and purification of Rab1a was performed as described previously (Machner and Isberg, 2006). For the purification of Rab4, Rab7, and Rab11, *Escherichia coli* strain BL21, transformed with a plasmid (pGEX4T-1) that contained the Rab, was grown at 37°C to an OD_{600} of 0.6. Protein expression was induced during an overnight incubation at 20°C in the presence of 1 mM isopropyl β-D-thiogalactoside. The next day, cells were harvested and resuspended in lysis buffer (PBS, 1 mM β-mercaptoethanol, 5 mM $MgCl_2$, and phenylmethylsulfonyl fluoride). The cells were lysed by sonication and centrifuged at 10,000 × *g* for 15 min. The cleared lysate was then loaded onto a glutathione-Sepharose column, washed extensively with lysis buffer, and eluted with lysis buffer containing 10 mM glutathione.

To preload Rabs with GDP, the Rabs were incubated at 30°C for 15 min in preloading buffer (50 mM Tris pH 8.0, 100 mM KCl, 1 mM EDTA, 1 mM DTT and 1 mg/ml BSA), then fivefold excess guanosine diphosphate (GDP) was added to the mixture. Nucleotide binding was stabilized by the addition of $MgCl_2$ (6 mM, final concentration) and then incubated for an additional 45 min. Free GDP was removed by a NAP-5 desalting column. For the guanosine triphosphate uptake assay, 10 pmol of [^{35}S]guanosine 5′-*O*-(3-thio)triphosphate(GTPγS) was added to 50 pmol of Rab-GDP in assay buffer (50 mM Tris, pH 7.5, 50 mM NaCl, 1 mM DTT, and 0.1 mM EDTA). Nucleotide exchange was initiated by transferring 8 pmol of the Rab to a tube containing the mTRAPP complex immobilized on beads. At the indicated time points, the reaction was stopped by the addition of ice-cold stop buffer (25 mM Tris, pH 8.0, and 20 mM $MgCl_2$). The reaction mixture was filtered through a nitrocellulose membrane (Millipore, Billerica, MA) and extensively washed with stop buffer. Protein-bound–radiolabeled nucleotide was retained on the membrane and measured by scintillation counting.

RESULTS

One Large Mammalian TRAPP Complex Can Be Detected by Gel Filtration Analysis

To begin to biochemically characterize mammalian TRAPP, we raised polyclonal antibodies to all known TRAPP homologues. Antibodies to five of the subunits (mTrs20, mBet3, mTrs23, mTrs120, and mTrs130) worked by Western blot analysis and were used in our studies. In yeast, Trs20p, Bet3p, and Trs23p are present in the TRAPPI and TRAPPII complexes, whereas Trs120p and Trs130p are only found in TRAPPII (Sacher *et al*., 2001). When we fractionated NIH3T3 cytosol on a Superdex-200 column, we could only detect one TRAPP complex in mammalian cells. This observation is consistent with the results reported by two other groups (Loh *et al*., 2005; Kummel *et al*., 2008). All TRAPP subunits analyzed cofractionated in fractions 9 and 10 with a predicted molecular mass of ~670 kDa (Figure 1A). This complex is approximately the size of the yeast TRAPPII complex (Sacher *et al*., 2001). Although a low-molecular-weight pool

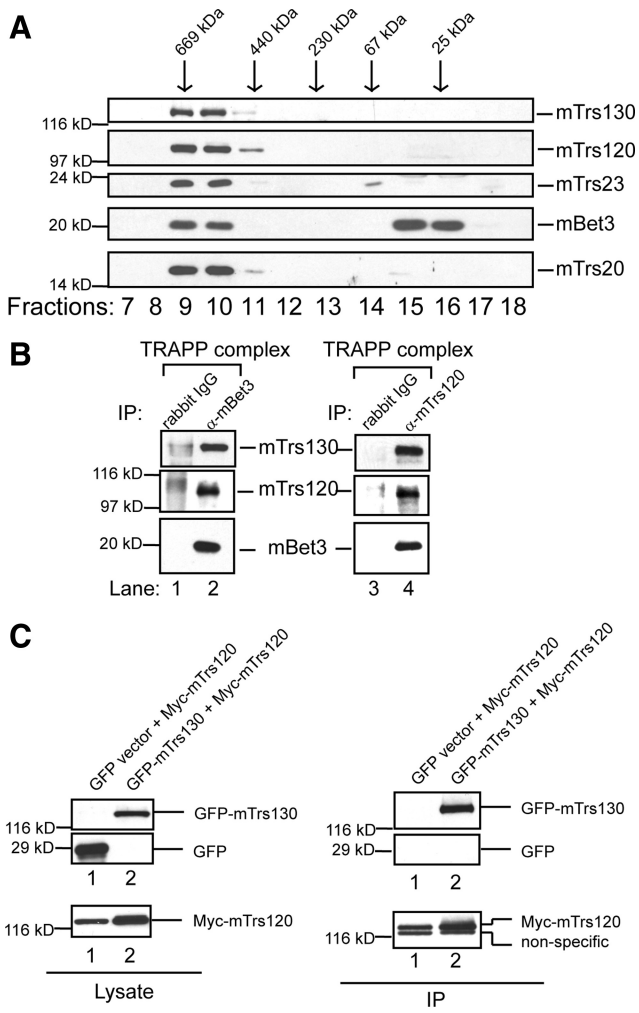

Figure 1. A mammalian TRAPPII complex is detected in NIH3T3 cells. (A) Cytosol from NIH3T3 cells was fractionated on a Superdex-200 gel filtration column. The column fractions were concentrated as described in the *Materials and Methods* and mTrs130, mTrs120, mTrs23, mBet3, and mTrs20 were detected by Western blot analysis. (B) Fractions 9 and 10 were pooled and immunoprecipitated with anti-mBet3 (left, lane 2) or anti-mTrs120 IgG (right, lane 4) to isolate the mammalian TRAPP complex. Coprecipitated TRAPP subunits were detected by Western blot analysis. Immunoprecipitation using nonspecific rabbit IgG was performed as a negative control (lanes 1 and 3). (C) mTrs120 interacts with mTrs130. A 10-cm plate of COS-7 cells, grown to 40% confluence, was transfected with 3 μg of plasmid DNA. The next day, the cells were washed with PBS and resuspended in 1 ml of lysis buffer (20 mM Tris, pH 7.5, 100 mM NaCl, 0.1% Triton X-100, 0.1% NP-40, and protease inhibitor cocktail). The lysed cells were spun at 16,000 × *g* for 10 min at 4°C in a microfuge tube. Lysates of COS-7 cells overexpressing GFP (SFNB 1520) and GFP-mTrs130 (SFNB 1173, left top two panels, lanes 1 and 2), or Myc-mTrs120 (SFNB 1517, left bottom panel, lanes 1 and 2) were processed for Western blot analysis using anti-GFP (top two panels) or anti-Myc (bottom) antibodies. The same lysates were also precipitated with anti-Myc antibody and blotted with either anti-GFP (right, top two panels) or anti-myc 9E10 (right, bottom) antibodies. Myc-mTrs120 only interacted with GFP-mTrs130 (right top, lane 2) and not with GFP (right middle, lane 1).

of mBet3 was also found in fractions 15 and 16, a smaller TRAPP complex the size of TRAPPI (~300 kDa) was not detected. A possible explanation for this observation is that TRAPPI may be far less abundant than TRAPPII in mammalian cells and is not detected by the methods we use here.

When fractions 9 and 10 were pooled, precipitated with anti-mBet3 antibody and blotted, mTrs130 and mTrs120 were present in the precipitate (Figure 1B, left). Conversely, when these column fractions were immunoprecipitated with an antibody directed against mTrs120, mBet3 and mTrs130 coprecipitated (Figure 1B, right). Similar results were obtained with anti-mTrs130 antibody (data not shown). Two other TRAPP subunits, mTrs23 and mTrs20, were also shown to coprecipitate in fractions 9 and 10 (data not shown). Therefore, based on subunit composition, these data indicate that Superdex-200 column fractions 9 and 10 contain a mammalian TRAPP complex that is analogous to yeast TRAPPII. Here, we address the role of mTRAPPII in membrane traffic.

Previously, we used two-hybrid analysis and in vitro binding studies to identify interactions among the small TRAPP subunits (Menon *et al*., 2006). This analysis did not include TRAPPII-specific subunits. For this reason, we wanted to address whether mTrs130 and mTrs120 directly interact with each other; however, we were unable to express these subunits in bacteria. To circumvent this problem, we coexpressed Myc-tagged full-length mTrs120 (Myc-mTrs120) and GFP-tagged full-length mTrs130 (GFP-mTrs130) in COS-7 cells (Figure 1C, left). Anti-Myc antibody (9E10) specifically coprecipitated Myc-mTrs120 with GFP-mTrs130, but not GFP (Figure 1C, right). We estimated that the 9E10 antibody precipitated >50% of the Myc-mTrs120 in the lysate and ~15% of the GFP-mTrs130. Although we cannot exclude the possibility that this is an indirect interaction, the high efficiency of coprecipitation of mTrs130 with mTrs120 is consistent with a direct interaction between these two proteins.

mTRAPPII Activates Rab1

mTRAPPII contains Bet3, which plays a pivotal role in catalyzing nucleotide exchange on Ypt1p (the yeast homologue of Rab1). Three other TRAPP subunits (Trs23p, Trs31p, and Bet5p) are also required for Ypt1p exchange activity (Kim *et al*., 2006; Cai *et al*., 2008), and the role that each of these subunits plays in catalyzing this activity has been described recently (Cai *et al*., 2008). The high degree of conservation among yeast and mammalian TRAPP subunits, and the recent finding that yeast TRAPPII is a Ypt1p GEF (Cai *et al*., 2008), prompted us to determine whether mTRAPPII, which contains mTrs130 and mTrs120, is a Rab1 GEF.

To address this possibility, we precipitated the complex from NIH3T3 lysate by using antibodies directed against the TRAPPII-specific subunits mTrs120 and mTrs130. This ensured that we specifically assayed the GEF activity of TRAPPII and not TRAPPI. Antibody injection experiments revealed that the anti-mTrs120 and mTrs130 antibodies, used in this study, did not inactivate the function of mTrs120 or mTrs130 (see *Materials and Methods*). Therefore, these antibodies should not inhibit GEF activity. For our studies, TRAPP containing protein A-Sepharose beads were washed extensively and then assayed at 25°C for their ability to stimulate guanine nucleotide exchange activity on Rab1. We found that mTRAPPII stimulated the guanine nucleotide exchange activity of Rab1 in a time-dependent manner (Figure 2A) but did not stimulate nucleotide exchange activity on Rab11 (Figure 2B), Rab4 (Supplemental Figure S1A) or Rab7 (Supplemental Figure S1B). The ability of mTRAPPII to stimulate the GEF activity of Rab11 (the yeast homologue of Ypt32p) was tested because it was recently suggested that the addition of Trs120p and Trs130p switches yeast TRAPP from a Ypt1p GEF to a Ypt32p GEF (Morozova *et al*., 2006). We, however, have found no evidence for this proposal with either mammalian or yeast TRAPPII (Cai *et al*., 2008). Approximately 0.018 pmol of mTRAPPII promoted the uptake of 0.4 pmol of GTPγS onto Rab1 in 20 min at 25°C, whereas no stimulation of GTPγS uptake was observed when the control beads were incubated without TRAPP, or when Rab1 was incubated with recombinant mBet3 (Figure 2A). We estimated, from multiple time points and experiments, that the intrinsic nucleotide exchange rate for Rab1 was 0.11 fmol/s. This rate was 0.32 fmol/s in the presence of mTRAPPII. The intrinsic nucleotide exchange rate for Rab11 was 0.26 fmol/s, and no stimulation of activity was observed when mTRAPPII was present. We conclude that the mammalian counterpart of yeast TRAPPII is a GEF that specifically activates Rab1 but not Rab11, Rab4, or Rab7.

Anti-mBet3 Antibody Blocks the Rab1 Guanine nucleotide exchange activity of mTRAPPII

We described previously an antibody to mBet3 that blocks homotypic COPII vesicle tethering in vitro and in vivo (Yu *et al*., 2006). The observation that yeast Bet3p plays a pivotal role in catalyzing nucleotide exchange on Ypt1p (Cai *et al*., 2008) raised the possibility that this antibody may disrupt membrane traffic by blocking Rab1 nucleotide exchange activity. To address this possibility, we fractionated lysate prepared from NIH3T3 cells on a Superdex-200 column. This separated the free pool of mBet3 from the pool that is part of the mTRAPPII complex (see fractions 9 and 10 in Figure 1A). Fractions containing mTRAPPII were precipitated with affinity-purified anti-mBet3 IgG, or anti-mTrs120 IgG, and blotted for the presence of mBet3. Although comparable amounts of mBet3 were precipitated with anti-mBet3 IgG and anti-mTrs120 IgG (Supplemental Figure S2, compare lanes 2 and 4), no stimulation of guanine nucleotide exchange activity on Rab1 was observed when mTRAPPII was precipitated with anti-mBet3 IgG (Figure 2C). In contrast, mTRAPPII still stimulated guanine nucleotide exchange activity on Rab1 (but not Rab11) when the complex was precipitated with anti-mTrs120 IgG (Figure 2, C and D) or anti-mTrs130 IgG (data not shown). Together, these findings indicate that the inactivation of mBet3 blocks the Rab1 GEF activity of mTRAPPII. They also show that mBet3 is required but not sufficient for Rab1 exchange activity (Cai *et al*., 2008), which is needed for COPII vesicle tethering (Bentley *et al*., 2006).

The TRAPPII-specific Subunit mTrs130 Largely Colocalizes with COPI

To begin to localize the counterpart of yeast TRAPPII in mammalian cells, we used indirect immunofluorescence microscopy to examine the localization of the TRAPPII-specific subunit mTrs130. We found that mTrs130 resides in the perinuclear region of COS-7 cells (Figure 3). Affinity-purified anti-mTrs130 antibody specifically recognized mTrs130, as these perinuclear structures were not observed when immunostaining was performed in the presence of recombinant mTrs130 (Supplemental Figure S3A). Because mTrs130 is a component of a Rab1 GEF, we colocalized mTrs130 with Rab1 and GM130. GM130 is a Rab1 effector that colocalizes with Rab1 on the *cis* side of the Golgi (Moyer *et al*., 2001; Satoh *et al*., 2003). mTrs130 partially colocalized with Rab1 (Figure 3A), GM130 (Figure 3B), and the COPI coat complex

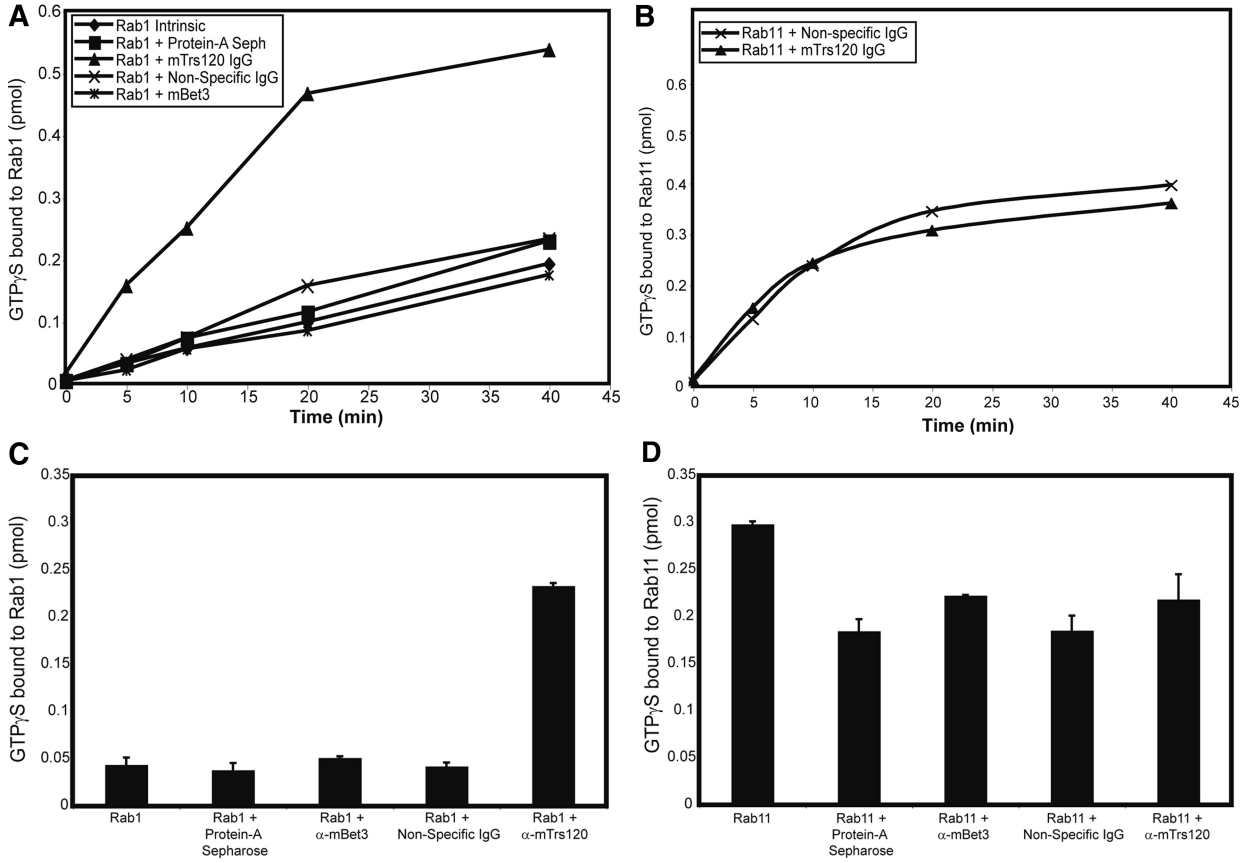

Figure 2. mTrs130 and mTrs120 are components of a TRAPPII complex that is a GEF for Rab1, but not Rab11. mTRAPPII was immunoprecipitated from NIH3T3 cytosol with anti-mTrs120 IgG, and its ability to stimulate guanine nucleotide exchange activity on Rab1a (A) or Rab11a (GeneID 8766) (B) was tested. Equal amounts of Superdex-200 column fractions 9 and 10 (Figure 1A), containing mTRAPPII, were immunoprecipitated with anti-mBet3 IgG, nonspecific rabbit IgG, or anti-mTrs120 IgG (also see Supplemental Figure S2). An equal volume of the protein A-Sepharose beads were then assayed 12 min for Rab1a (C) or Rab 11a (D) guanine nucleotide exchange activity. Similar results were obtained when the complex was precipitated with anti-mTrs130 antibody (data not shown). Error bars are SEM.

(Figure 3C), which is recruited to Golgi membranes (Moelleken *et al*., 2007). mTrs130 also partially colocalized with the pre-Golgi marker ERGIC-53 (Supplemental Figure S3B), but not Sec31A (Supplemental Figure S3C), a marker for the tER (Barlowe *et al*., 1994). mTrs130 did not colocalize with the TGN marker γ-adaptin (Supplemental Figure S3D), but some mTrs130 was observed at *trans*-Golgi membranes marked by GalT (Figure 3D).

To analyze the localization of mTrs130 in greater detail, we treated COS-7 cells with nocodazole, a microtubule-depolymerizing agent that disperses the compartments of the ER-Golgi pathway into small punctate structures (Cole *et al*., 1996). In nocodazole-treated cells, mTrs130 partially colocalized with Rab1 (Figure 4A), GM130 (Figure 4B) and COPI (Figure 4C), and to a lesser extent with ERGIC-53 (Supplemental Figure S4A) and GalT (Figure 4D). In addition, mTrs130 was adjacent to γ-adaptin (Supplemental Figure S4B), and Sec31A clustered near mTrs130 (Supplemental Figure S4C). tER sites are known to cluster near Golgi fragments in nocodazole treated cells (Hammond and Glick, 2000). Consistent with the proposal that mTrs130 extensively colocalizes with early Golgi membranes, we found that its localization was sensitive to BFA (Supplemental Figure S5, bottom left). BFA is a drug that dissociates the COPI coat from Golgi membranes (Supplemental Figure S5, bottom right) and redistributes Golgi glycosylation enzymes to the ER (Ward *et al*., 2001). Together, these findings indicate that the mammalian homologue of the yeast TRAPPII-specific subunit Trs130p predominantly resides on early Golgi structures and not the TGN.

mTRAPPII Is Enriched on Peripheral COPI-coated Vesicles and Buds

If Superdex-200 column fractions 9 and 10 contain a TRAPP complex that is analogous to yeast TRAPPII, then other TRAPP subunits that are largely found in these fractions also should colocalize with early Golgi markers similar to mTrs130. We found that both anti-mTrs23 and anti-mTrs20 antibodies worked by immunofluorescence. Like mTrs130, mTrs23 was found to be sensitive to BFA (data not shown) and largely colocalized with GM130 and COPI in the absence (Figure 5, A and B) and presence of nocodazole (Supplemental Figure S6, B and C). Similar results were obtained with anti-mTrs20 antibody, although this antibody also nonspecifically labeled the nucleus (data not shown).

Although our immunofluorescence data implies that mTRAPPII largely resides on early Golgi membranes, these experiments do not address whether mTRAPPII is present on Golgi cisternae. To address this question, quantitative immuno-EM studies were performed. Of the anti-TRAPP antibodies used in this study, only mTrs23 worked by immuno-EM. Using antibodies directed against anti-mTrs23 and the COPI subunit β′COP (Figure 5C), multiple grids were examined and profiles of Golgi areas were recorded

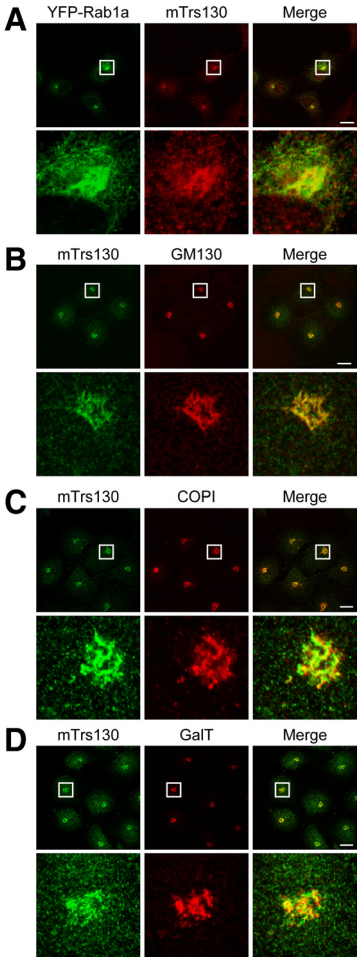

Figure 3. mTrs130 largely colocalizes with early Golgi markers. Colocalization experiments were performed in COS-7 cells with antibodies directed to mTrs130 (red) and YFP-Rab1a (green) (A), mTrs130 (green) and GM130 (red) (B), mTrs130 (green) and COPI (red) (C), and mTrs130 (green) and the *trans*-Golgi marker GalT (red) (D). The images were captured on a scanning laser confocal microscope using a 63× objective lens. The merged images are shown on the right, and the insets are magnified in the next row. Bar, 20 μm.

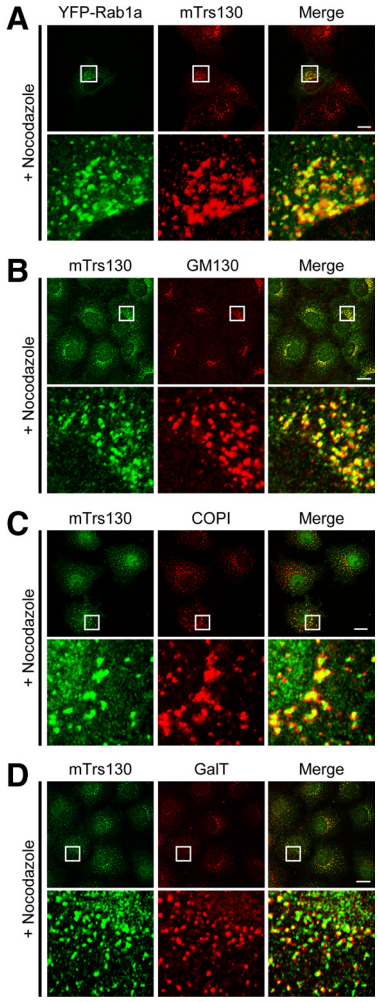

Figure 4. mTrs130 colocalizes with GM130 and COPI in nocodazole treated cells. COS-7 cells were treated with 10 μg/ml nocodazole for 1 h before the samples were fixed and processed for staining with antibodies directed against mTrs130 (red) and YFP-Rab1a (green) (A), mTrs130 (green) and GM130 (red) (B), mTrs130 (green) and COPI (red) (C), and mTrs130 (green) and GalT (red) (D). The merged images are shown on the right, and the insets are magnified in the next row. Bar, 20 μm.

and grouped. Gold particles on ER, pre-Golgi membranes, and the TGN were also counted. It is interesting that this analysis revealed that Golgi-associated mTrs23 is predominantly found on the rims of Golgi cisternae and vesicular profiles located at the Golgi periphery (Figure 5, C and D). These rims and vesicles also contained the COPI subunit β'COP (Figure 5C). Quantitation revealed that ~74% of the mTrs23-labeled gold particles were present on peripheral vesicles and buds in the Golgi area (Figure 5D); 71% of the β'COP also localized to peripheral vesicles and buds (Figure 5E). In addition, ~1/3 of the mTrs23 positive peripheral vesicles and buds contained β'COP. Together, these findings indicate that the membrane-bound pool of mTRAPPII is bound to COPI coated vesicles and not Golgi cisternae.

mTRAPPII Interacts with γ1COP

Studies in yeast suggested that TRAPPII-specific subunits may play a role in tethering COPI-coated vesicles to the Golgi. Specifically, TRAPP bound to the COPI coat complex in yeast lysates, and COPI-coated vesicles were mislocalized in *trs120* mutants (Cai *et al*., 2005). Earlier studies did not address whether TRAPPII-specific subunits bound to the COPI coat complex, nor did they identify a subunit of the COPI coat that interacts with TRAPPII. The localization of mTRAPPII to COPI-coated vesicles prompted us to determine whether mTrs130 and mTrs120 interact with subunits of the COPI coat complex. The COPI complex is composed of two subcomplexes (Boehm and Bonifacino, 2001). The F1-COPI subcomplex contains the β, γ, δ, and ζ subunits, which are homologous to the adaptins, the clathrin cargo adaptor proteins. The B-COPI subcomplex contains the remaining subunits (α, β', and ε), which may be functionally equivalent to clathrin.

Previous studies have shown that the yeast TRAPPI complex must directly interact with the COPII cargo adaptor complex to tether COPII vesicles (Cai *et al*., 2007b). Therefore, to begin to determine whether mTRAPPII interacts with the COPI coat, we focused on the subunits of the putative cargo adaptor complex. For this analysis, we coex-

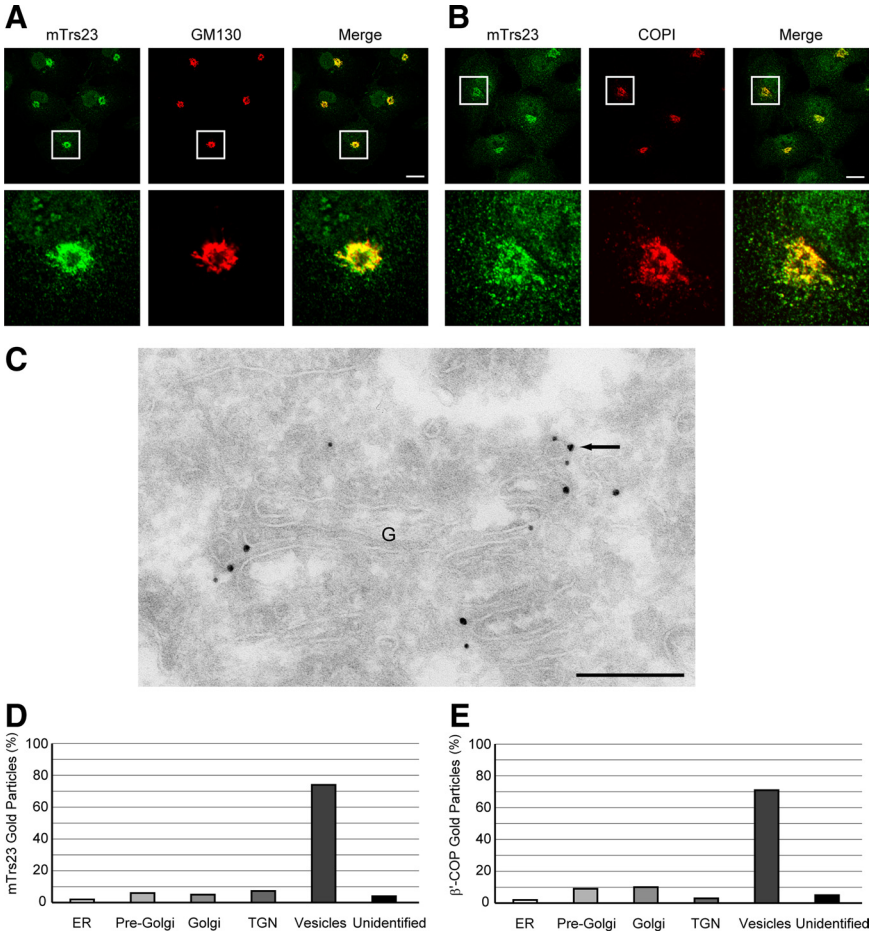

Figure 5. The mTRAPPII complex is bound to COPI-coated vesicles. mTrs23 (green) colocalizes with GM130 (red) (A) and COPI (red) in COS-7 cells (B). (C) Immuno-EM was performed in NRK cells by using anti-mTrs23 and anti-β′COP antibodies as described in *Materials and Methods*. The arrow points to a COPI coated bud that contains mTrs23 (15-nm gold particles) and β′COP (10-nm gold particles). G denotes Golgi cisternae. Bar, 200 nm. (D and E) Multiple grids dual-labeled for mTrs23 and β′COP were quantitated as described in *Materials and Methods*. The data for mTrs23 is shown in D and β′COP in E.

pressed GFP-mTrs130, or Myc-mTrs120, with hemagglutinin (HA)-tagged COPI subunits in COS-7 cells. The following subunits were tested: β, γ1, γ2, δ, and ζ1 and the ε subunit of B-COPI. There are two forms of γCOP, γ1 and γ2. Quantitative immuno-EM revealed that γ1 preferentially localizes to the *cis*-side of the Golgi, whereas γ2 is predominantly on the *trans*-side (Moellekan *et al*., 2007). Of all the tagged COPI subunits that were tested (β, γ1, γ2, δ, and ζ1 and the ε subunit of B-COPI), only γ1 and εCOP were expressed. It is interesting that we found that GFP-mTrs130 and Myc-mTrs120 interacted with γ1COP, but not εCOP (Figure 6, A and B, lanes 2 and 3, compared with lysate in lanes 5 and 6). This interaction seemed to be specific because mBet3, which is known to bind to the COPII coat adaptor complex (Cai *et al*., 2007a), does not bind to γ1COP (Figure 6, A and B, lane 1, compared with lysate in lane 4). We estimated that ~1.3% of the GFP-mTrs130 in the lysate coprecipitated with 40% of the HA-γ1COP, whereas 8.2% of the Myc-mTrs120 in the lysate coprecipitated with 37% of the HA-γ1COP.

The amino terminus of γ1COP, but not the carboxy terminus, interacts with the dilysine motif of cargo (Harter and Wieland, 1998; Wu *et al*., 2000). To determine whether this region of γ1COP specifically interacts with mTrs120 and mTrs130, we expressed GFP-mTrs120 and GFP-mTrs130 in COS-7 cells and compared their ability to bind to purified recombinant GST-γ1COP (amino acids 1-607) and GST-γ1COP (amino acids 608-874). As a control, we also expressed GFP-mBet3 in COS-7 cells and assessed its ability to bind to both GST-γ1COP constructs. It is interesting that ~8.4% of the GFP-mTrs120 in the binding reaction bound to GST-γ1COP (1-607), but not GST or GST-γ1COP (608-874) (Figure 6C, middle lanes 1–3 compared with lane 4). This interaction seemed to be specific because no interaction was detected with GFP-mBet3 (Figure 6C, bottom lanes 1–3 compared with lane 4). Weaker binding (~2.2% of the input lysate) also was observed with GFP-mTrs130 (Figure 6C, top lanes 1–3 compared with lane 4). Thus, the TRAPPII-specific subunits mTrs120 and mTrs130 specifically interact with the amino terminus of γ1COP, a putative cargo adaptor subunit of the COPI coat complex (Boehm and Bonifacino, 2001). The high efficiency of the interaction between mTrs120 and γ1COP is consistent with a direct interaction between these two proteins. Because mTrs120 and mTrs130 seem to interact with each other, the less efficient interaction of mTrs130 with γ1COP may be either direct or through mTrs120.

mTrs130 Is Required for Golgi Architecture and Early Golgi Traffic

To begin to address where mTrs130 functions, we transfected COS-7 cells with two different shRNA expression vectors (vector 1 and vector 2) that target mTrs130 mRNA at different positions (see *Materials and Methods*). We found that, in contrast to mock treated cells, shRNA-treated cells were depleted of mTrs130, but not the ER protein ER60 (Figure 7A). Western blot analysis revealed that mTrs130 was reduced ~76.4 ± 8.7% with vector 1 and ~51.2 ± 11.3% with vector 2. The loss of mTrs130 disrupted early Golgi membranes that colocalized with COPI (data not shown)

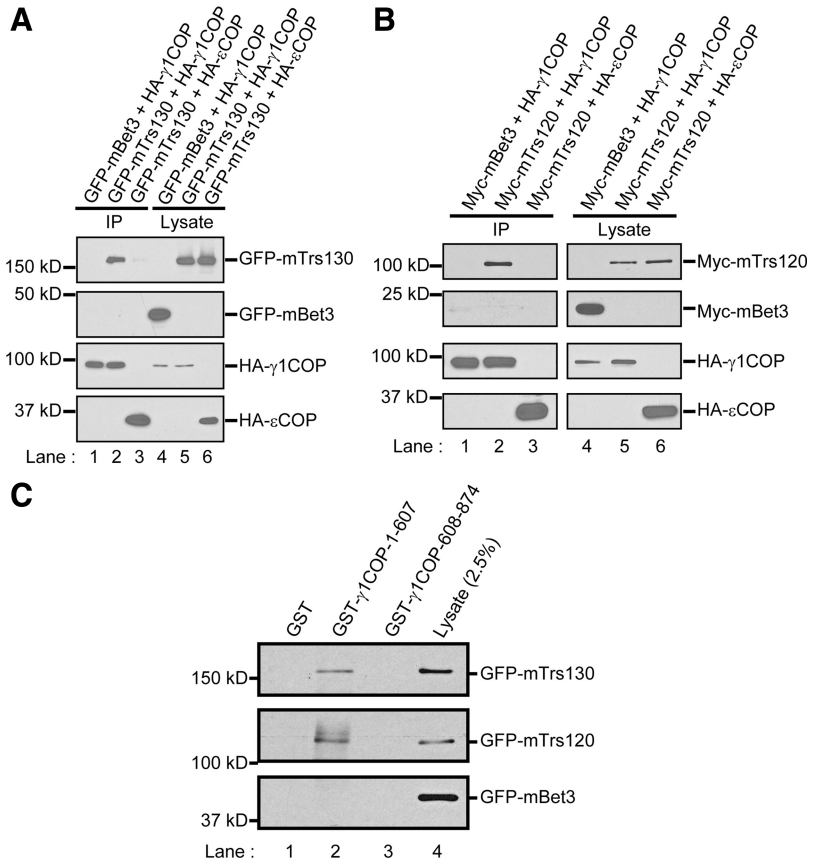

Figure 6. mTRAPPII interacts with γ1COP. mTrs130 (A) and mTrs120 (B) coprecipitate with HA-γ1COP. The protocol used to immunoprecipitate HA-γ1COP was the same as described in the legend to Figure 1C only the cells were lysed in 50 mM Tris, pH 7.4, 100 mM NaCl, 1 mM EDTA, 1% NP-40 (plus protease inhibitor cocktail). HA-γ1COP was precipitated by incubating 1.8–2.5 mg of lysate with anti-HA–conjugated beads (10 μl). The beads were washed three times with 50 mM Tris, pH 7.4, 100 mM NaCl, 1 mM EDTA, 0.5% NP-40 and processed for Western blot analysis. The precipitate (40% of the sample) and lysate (1% of the sample) were blotted with anti-GFP antibody (top left), anti-myc antibody (top right) or anti-HA antibody (bottom). GFP-mTrs130 interacted with γ1COP but not εCOP (Figure 6A, lanes 2 and 3, compare to lysate in lanes 5 and 6). Myc-mTrs120 interacted with γ1COP but not εCOP (Figure 6B, lanes 2 and 3, compare to lysate in lanes 5 and 6). The interaction with γ1COP was specific, because mBet3 did not interact with γ1COP (Figure 6, A and B, lane 1, compared with lysate in lane 4). (C) Binding assays were done as described in Cai *et al*. (2007b), with the following modifications. Sixty microliters of beads (2 μg of fusion protein) were incubated overnight at 4°C with 0.8 mg of lysate in a reaction volume of ~200 μl. Half of the binding reaction was loaded onto the gel.

and GM130 (Figure 7B). This defect was due to the loss of mTrs130, as it was prevented by the expression of a GFP-mTrs130 construct (GFP-mTrs130*) that harbored three silent base changes (see *Materials and Methods*) in the sequence targeted by the shRNA expression vector1 (Figure 7C). Similar results were obtained with shRNA expression vector 2 (data not shown).

EM analysis confirmed that the depletion of mTrs130 disrupts the architecture of the Golgi (Figure 8A, compare the Golgi [G] in the top and bottom micrographs), and leads to an accumulation of vesicles (50–80 nm) in the vicinity of the Golgi complex (see filled arrows in Figure 8A, top). Quantitation of the data revealed a twofold increase in the number of vesicles that accumulate in the Golgi area (Figure 8B) and a twofold decrease in the amount of membrane that represents Golgi cisternae in the mTrs130-depleted cells (Figure 8C).

To determine whether mTrs130 is required for Golgi traffic, we transfected mock-treated and mTrs130-depleted cells at 37°C with a plasmid that expresses tsO45 VSV-G-GFP. Twenty-four hours after transfection, the cells were incubated at 42°C to accumulate misfolded tsO45 VSV-G-GFP in the ER. Cycloheximide was added and the cells were shifted to 32°C for 30, 60, and 90 min. At 32°C, tsO45 VSV-G-GFP folds into a conformation that is compatible with export from the ER. The trafficking of VSV-G to the cell surface was monitored at this temperature by immunofluorescence (Figure 9A) by using an antibody to the ectodomain of VSV-G as described previously (Diao *et al*., 2003). The delivery of VSV-G to the cell surface was blocked in the mTrs130-depleted cells, but not the mock-treated cells (Figure 9). The VSV-G that failed to be delivered to the surface in the mTrs130-depleted cells largely colocalized with GM130 (Figure 9B, compare mock and shRNA-treated cells) and not the TGN marker γ-adaptin (Supplemental Figure S7). To assess whether the loss of mTrs130 disrupts ER-Golgi traffic, we examined the trafficking of VSV-G at earlier times in the mTrs130-depleted cells. By 10 min, VSV-G reached the Golgi in both mock and depleted cells (see filled arrows in Supplemental Figure S8). Approximately 30 cells were examined and no significant delay in ER–Golgi traffic was observed. Additionally, no significant delay was observed in the trafficking of the transmembrane protein ERGIC-53 (Schindler *et al*., 1993) from the ER to the pre-Golgi compartment (data not shown). Together, these findings imply that mTrs130 mediates early Golgi traffic and not ER–Golgi transport.

DISCUSSION

Although a mammalian homologue of the TRAPPII-specific subunit Trs130p was identified years ago (Sacher *et al*., 2000), the role of mTrs130 and mTRAPPII in membrane traffic has not been addressed. Here, we show that mTrs130 is a component of a GEF that activates Rab1, but not Rab11, Rab7, or Rab4. We also show that in the absence of mTrs130, Golgi architecture is disrupted and anterograde early Golgi traffic is blocked. These results are consistent with earlier studies showing that membrane traffic between the *cis*- and *medial*-Golgi is Rab1 dependent (Plutner *et al*., 1991) and that Rab1 is required for the maintenance of a functional Golgi (Wilson *et al*., 1994; Haas *et al*., 2007).

Gel filtration analysis of an NIH3T3 lysate revealed that mTrs130 is a component of an ~670-kDa complex that includes mTrs120, and the small mTRAPP subunits mBet3, mTrs23, and mTrs20. mTrs130, mTrs20, and mTrs23 also

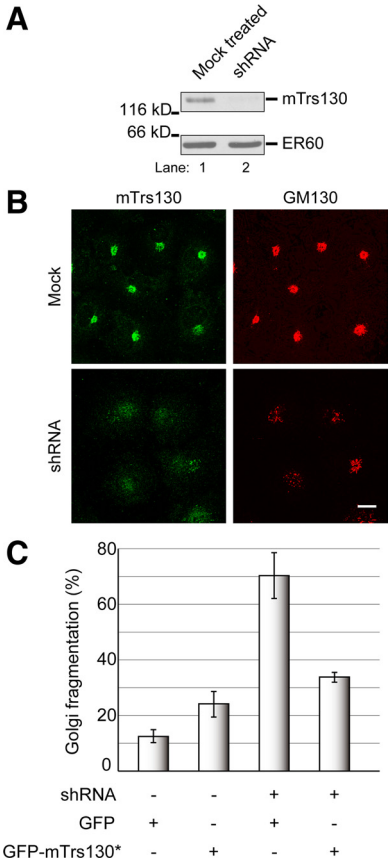

Figure 7. The depletion of mTrs130 disrupts the early Golgi. (A) COS-7 cells were transfected with the pSilencer 1.0-U6 vector (mock) or vector1 (shRNA). The cells were harvested 48 h after transfection and immunoblotted with anti-Trs130 (top) and anti-ER60 antibodies (bottom). The ER protein ER60 was used as a loading control. (B) COS-7 cells were transfected with pSilencer 1.0-U6 vector (mock) or vector1 (shRNA) and immunostained with anti-mTrs130 (green) and anti-GM130 antibodies (red). (C) COS-7 cells were transfected with the pSilencer 1.0-U6 vector (mock) or vector1 (shRNA) together with vectors that express either GFP or GFP-mTrs130* (see *Materials and Methods*). The cells were immunostained with anti-GM130 antibody and the number of fragmented Golgi was quantitated in greater than 30 cells. SEM was calculated from three independent experiments. Bar, 20 μm.

largely colocalize with the early Golgi markers GM130 and COPI. Thus, all mTRAPP subunits analyzed to date, with the exception of mBet3 (Yu *et al*., 2006), display the same localization. Gel filtration analysis shows two pools of mBet3 in NIH3T3 lysates, a low-molecular-weight and a high-molecular-weight pool. We speculate that the low-molecular-weight pool of mBet3, which seems to be inactive (our unpublished observations), resides at the tER. This pool of mBet3 may direct complex assembly at this site. Previous studies have shown that some mBet3 also colocalizes with early Golgi markers (Yu *et al*., 2006), consistent with the observation that it is a component of the high-molecular-weight mTRAPPII complex. These data support the hypothesis that mTRAPPII is analogous to the yeast TRAPPII complex. We hypothesize that the smaller TRAPPI complex is less abundant in mammalian cells and is not detected by the methods we have used in this study.

Our studies have shown that the loss of mTrs130 and mBet3 lead to different phenotypes. Antibody inhibition experiments and RNA interference studies revealed that

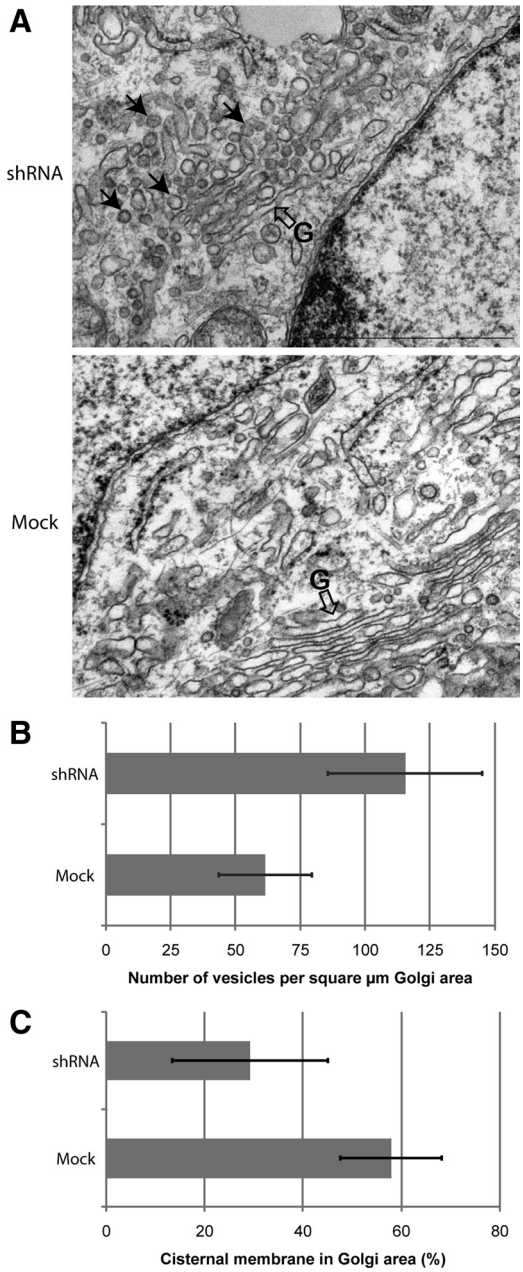

Figure 8. The depletion of mTrs130 by shRNA leads to the accumulation of vesicles in the vicinity of the Golgi. (A) After depleting cells of mTrs130 by shRNA expression vector1, the cells were fixed and processed for EM as described in the *Materials and Methods*. A representative EM micrograph of mTrs130-depleted cells is shown at the top of the figure, and the mock-treated cells are shown at the bottom. Empty arrows point to Golgi cisternae and filled arrows to vesicles in the vicinity of the Golgi. (B) Quantitation of the number of vesicles per square μm of Golgi area in the shRNA and mock-treated cells. (C) Quantitation of Golgi cisternal membranes in shRNA and mock-treated cells. $p < 0.0001$. Bar, 1 μm.

mBet3 is required for ER–Golgi traffic in vivo (Yu *et al*., 2006). When mBet3 function is disrupted, anterograde traffic is blocked and cargo accumulates in COPII-coated membranes. In vitro, mBet3 is required for homotypic COPII vesicle tethering and fusion (Yu *et al*., 2006). COPII vesicle tethering and fusion also requires the GTPase Rab1 (Bentley *et al*., 2006). Like yeast Bet3p, we show here that mBet3 is

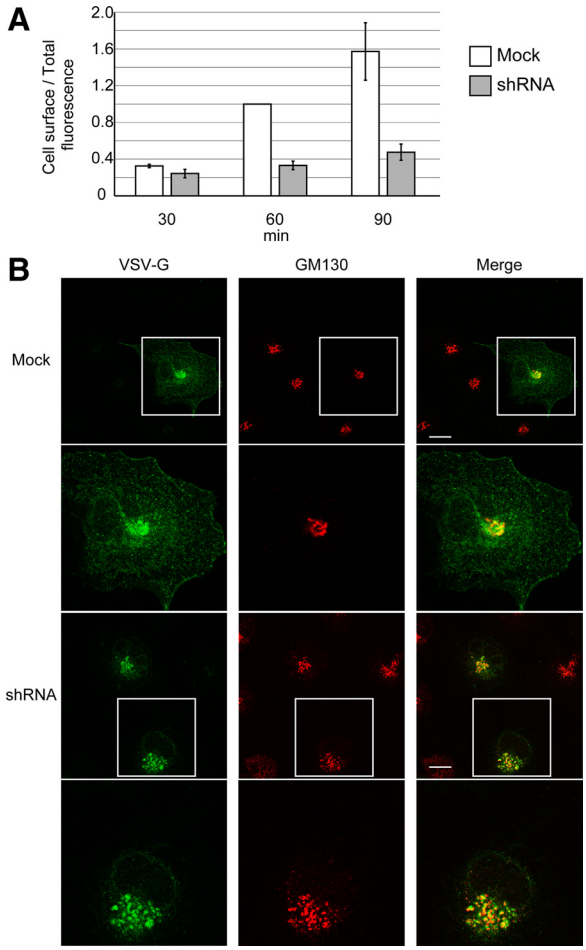

Figure 9. The depletion of mTrs130 leads to the accumulation of VSV-G in an early Golgi compartment that is marked by GM130. (A) To express tsO45VSV-G-GFP, pEGFPN1-VSV-G was cotransfected with the pSilencer 1.0-U6 (mock) vector or vector1 (shRNA). The cells were incubated at 40°C for 20 h, cycloheximide was added, and 30 min later the cells were shifted to 32°C for 30, 60, and 90 min. To detect cell surface VSV-G-GFP, the cells were fixed without permeabilization and immunostained with anti-VSV-G antibody. The data shown was quantitated from four independent experiments as described in the *Materials and Methods*. Greater than 30 cells were quantified in each experiment. The 60-min time point was set to one. Error bars are the SEM. (B) The protocol was the same as in A, only the 90-min samples were fixed and permeabilized with methanol. The cells were immunostained with anti-GM130 antibody (red). VSV-G was detected with a GFP tag (green). Greater than 58 cells were quantified in three independent experiments.

needed but is not sufficient for Rab1 GEF activity. In contrast to the phenotypes observed for the loss of mBet3 function, we found that the depletion of mTrs130 disrupts Golgi traffic; as a consequence, cargo accumulates in the early Golgi.

TRAPP interacts with the COPI coat complex in yeast lysates, and COPI vesicles are mislocalized in *trs120* mutants (Cai *et al*., 2005). These findings and the observation that TRAPPI, but not TRAPPII, binds to COPII vesicles (Sacher *et al*., 2001), led to the proposal that TRAPPII-specific subunits may mask the COPII binding site on Bet3 to convert this Ypt1p/Rab1 GEF into a tether that specifically recognizes COPI vesicles (Cai *et al*., 2008). In the present study, we provide the first direct evidence for this proposal by demonstrating that mTRAPPII localizes to COPI-coated vesicles and buds and binds to γ1COP, which is enriched on the *cis*-side of the Golgi (Moelleken *et al*., 2007). The observation that mTrs120 efficiently coprecipitates with γ1COP fits well with studies in yeast that showed COPI-coated vesicles are mislocalized in *trs120* mutants (Cai *et al*., 2005). Consistent with a role for mTRAPPII in tethering COPI vesicles, we show that when anterograde early Golgi traffic is blocked in mTrs130-depleted cells, vesicles accumulate in the vicinity of the Golgi. We propose that mTRAPPII is both a tether and a GEF. The TRAPPII-specific subunits, mTrs130 and mTrs120 mediate tethering functions, whereas essential TRAPP subunits that are present in both yeast TRAPPI and TRAPPII (Bet3, Trs23, Trs31, and Bet5) are required for Rab1 GEF activity.

It is interesting that although the yeast TRAPPII complex is a Ypt1p (Rab1) GEF (Cai *et al*., 2008), it largely resides on the late Golgi and mediates traffic throughout the Golgi, including the late Golgi (Cai *et al*., 2005). This is different from what we report here for mTrs130, which largely colocalizes with early Golgi markers. mTrs130 is also required for early Golgi traffic and does not seem to be needed for membrane traffic at the TGN. Although the components of the secretory apparatus are highly conserved, differences in the architecture of the ER–Golgi pathway between yeast and mammals could explain why TRAPPII seems to localize and function in different compartments in lower and higher eukaryotes. Our findings imply that the GTPase Ypt1p regulates the flow of traffic into the *cis* - and *trans*-sides of the yeast Golgi, whereas Rab1 regulates traffic into the *cis*-face of the Golgi. In mammals, a related Rab family member may regulate traffic into the *trans*-Golgi.

ACKNOWLEDGMENTS

We thank Martina Medkova for advice on Rab nucleotide exchange assays, Craig Roy, Ralph Isberg, David Lambright, Fred Gorelick, Hans-Peter Hauri, Cathy Jackson, Rick Cerione, Rainer Pepperkok, David Shima, Yu Yamaguchi, and Graham Warren for plasmids and other reagents, and Emi Mizuno-Yamasaki for a critical reading of the manuscript. We thank George Patterson and Jennifer Lippincott-Schwartz for plasmid pEGFPdKA206K-N1-VSVG tsO45, Christina Horensavitz and Christoph Rahner in the Yale EM facility for technical assistance, and the late Marc Pypaert for advice. We thank Mark von Peski and René Scriwanek for assistance with the preparation of the cryosection electron micrographs. We also thank the Department of Cellular and Molecular Medicine, Electron Microscopy Facility at University of California–San Diego, headed by Marilyn Farquhar, for quantitation of the immuno-EM. This work was supported by the Howard Hughes Medical Institute. Salary support for A. Y., S. M., S. Y., J. B., and S.F.-N. was provided by the Howard Hughes Medical Institute. Salary support for Ayano Satoh was provided by National Institutes of Health grant 1R03AG030101-01A1 and 5R01GM060919-08.

REFERENCES

Allan, B. B., Moyer, B. D., and Balch, W. E. (2000). Rab1 recruitment of p115 into a cis-SNARE complex: programming budding COPII vesicles for fusion. Science *289*, 444–448.

Aridor, M., Bannykh, S. I., Rowe, T., and Balch, W. E. (1995). Sequential coupling between COPII and COPI vesicle coats in endoplasmic reticulum to Golgi transport. J. Cell Biol. *131*, 875–893.

Barlowe, C., Orci, L., Yeung, T., Hosobuchi, M., Hamamoto, S., Salama, N., Rexach, M. F., Ravazzola, M., Amherdt, M., and Schekman, R. (1994). COPII: a membrane coat formed by Sec proteins that drive vesicle budding from the endoplasmic reticulum. Cell *77*, 895–907.

Beard, M., Satoh, A., Shorter, J., and Warren, G. (2005). A cryptic Rab1-binding site in the p115 tethering protein. J. Biol. Chem. *280*, 25840–25848.

Bentley, M., Liang, Y., Mullen, K., Xu, D., Sztul, E., and Hay, J. C. (2006). SNARE status regulates tether recruitment and function in homotypic COPII vesicle fusion. J. Biol. Chem. *281*, 38825–38833.

Boehm, M., and Bonifacino, J. S. (2001). Adaptins: the final recount. Mol. Biol. Cell *12*, 2907–2920.

Bonifacino, J. S., and Lippincott-Schwartz, J. (2003). Coat proteins: shaping membrane transport. Nat. Rev. Mol. Cell Biol. *4*, 409–414.

Cai, H., Reinisch, K., and Ferro-Novick, S. (2007a). Coats, tethers, Rabs, and SNAREs work together to mediate the intracellular destination of a transport vesicle. Dev. Cell *12*, 671–682.

Cai, H., Yu, S., Menon, S., Cai, Y., Lazarova, D., Fu, C., Reinisch, K., Hay, J. C., and Ferro-Novick, S. (2007b). TRAPPI tethers COPII vesicles by binding the coat subunit Sec23. Nature *445*, 941–944.

Cai, H., Zhang, Y., Pypaert, M., Walker, L., and Ferro-Novick, S. (2005). Mutants in trs120 disrupt traffic from the early endosome to the late Golgi. J. Cell Biol. *171*, 823–833.

Cai, Y., Chin, H. F., Lazarova, D., Menon, S., Fu, C., Cai, H., Sclafani, A., Rodgers, D. W., De La Cruz, E. M., Ferro-Novick, S., and Reinisch, K. M. (2008). The structural basis for activation of the Rab Ypt1p by the TRAPP membrane-tethering complexes. Cell *133*, 1202–1213.

Cole, N. B., Smith, C. L., Sciaky, N., Terasaki, M., Edidin, M., and Lippincott-Schwartz, J. (1996). Diffusional mobility of Golgi proteins in membranes of living cells. Science *273*, 797–801.

Davidson, H. W., and Balch, W. E. (1993). Differential inhibition of multiple vesicular transport steps between the endoplasmic reticulum and trans Golgi network. J. Biol. Chem. *268*, 4216–4226.

Diao, A., Rahman, D., Pappin, D. J., Lucocq, J., and Lowe, M. (2003). The coiled-coil membrane protein golgin-84 is a novel rab effector required for Golgi ribbon formation. J. Cell Biol. *160*, 201–212.

Haas, A. K., Yoshimura, S., Stephens, D. J., Preisinger, C., Fuchs, E., and Barr, F. A. (2007). Analysis of GTPase-activating proteins: Rab1 and Rab43 are key Rabs required to maintain a functional Golgi complex in human cells. J. Cell Sci. *120*, 2997–3010.

Hammond, A. T., and Glick, B. S. (2000). Dynamics of Transitional Endoplasmic Reticulum Sites in Vertebrate Cells. Mol. Biol. Cell *11*, 3013–3030.

Harter, C., and Wieland, F. T. (1998). A single binding site for dilysine retrieval motifs and p23 within the gamma subunit of coatomer. Proc. Natl. Acad. Sci. USA *95*, 11649–11654.

Kim, Y.-G., Raunser, S., Munger, C., Wagner, J., Song, Y.-L., Cygler, M., Walz, T., Oh, B.-H. and Sacher, M. (2006). The architecture of the multisubunit TRAPP I complex suggests a model for vesicle tethering. Cell *127*, 817–830.

Kuehn, M. J., Herrmann, J. M., and Schekman, R. (1998). COPII-cargo interactions direct protein sorting into ER-derived transport vesicles. Nature *391*, 187–190.

Kummel, D., Oeckinghaus, A., Wang, C., Krappmann, D., and Heinemann, U. (2008). Distinct isocomplexes of the TRAPP trafficking factor coexist inside human cells. FEBS Lett. *582*, 3729–3733.

Liou, W., Geuze, H. J., and Slot, J. W. (1996). Improving structural integrity of cryosections for immunogold labeling. Histochem. Cell Biol. *106*, 41–58.

Loh, E., Peter, F., Subramaniam, V. N., and Hong, W. (2005). Mammalian Bet3 functions as a cytosolic factor participating in transport from the ER to the Golgi apparatus. J. Cell Sci. *118*, 1209–1222.

Machner, M. P., and Isberg, R. R. (2006). Targeting of host Rab GTPase function by the intravacuolar pathogen *Legionella pneumophila*. Dev. Cell *11*, 47–56.

Menon, S., Cai, H., Lu, H., Dong, G., Cai, Y., Reinisch, K., and Ferro-Novick, S. (2006). mBET3 is required for the organization of the TRAPP complexes. Biochem. Biophys. Res. Commun. *350*, 669–677.

Moelleken, J., *et al*. (2007). Differential localization of coatomer complex isoforms within the Golgi apparatus. Proc. Natl. Acad. Sci. USA *104*, 4425–4430.

Morozova, N., Liang, Y., Tokarev, A. A., Chen, S. H., Cox, R., Andrejic, J., Lipatova, Z., Sciorra, V. A., Emr, S. D., and Segev, N. (2006). TRAPPII subunits are required for the specificity switch of a Ypt-Rab GEF. Nat. Cell Biol. *8*, 1263–1269.

Moyer, B. D., Allan, B. B., and Balch, W. E. (2001). Rab1 interaction with a GM130 effector complex regulates COPII vesicle cis–Golgi tethering. Traffic *2*, 268–276.

Patterson, G. H., Hirschberg, K., Polishchuk, R. S., Gerlich, D., Phair, R. D., and Lippincott-Schwartz, J. (2008). Transport through the Golgi apparatus by rapid partitioning within a two-phase membrane system. Cell *133*, 1055–1067.

Pfeffer, S. R. (1999). Transport-vesicle targeting: tethers before SNAREs. Nat. Cell Biol. *1*, E17–E22.

Plutner, H., Cox, A. D., Pind, S., Khosravi-Far, R., Bourne, J. R., Schwaninger, R., Der, C. J., and Balch, W. E. (1991). Rab1b regulates vesicular transport between the endoplasmic reticulum and successive Golgi compartments. J. Cell Biol. *115*, 31–43.

Sacher, M., Barrowman, J., Schieltz, D., Yates, J. R., 3rd and Ferro-Novick, S. (2000). Identification and characterization of five new subunits of TRAPP. Eur. J. Cell Biol. *79*, 71–80.

Sacher, M., Barrowman, J., Wang, W., Horecka, J., Zhang, Y., Pypaert, M., and Ferro-Novick, S. (2001). TRAPP I implicated in the specificity of tethering in ER-to-Golgi transport. Mol. Cell *7*, 433–442.

Satoh, A., Wang, Y., Malsam, J., Beard, M. B., and Warren, G. (2003). Golgin-84 is a rab1 binding partner involved in Golgi structure. Traffic *4*, 153–161.

Schindler, R., Itin, C., Zerial, M., Lottspeich, F., and Hauri, H. P. (1993). ERGIC-53, a membrane protein of the ER-Golgi intermediate compartment, carries an ER retention motif. Eur. J. Cell Biol. *61*, 1–9.

Seemann, J., Jokitalo, E. J., and Warren, G. (2000). The role of the tethering proteins p115 and GM130 in transport through the Golgi apparatus in vivo. Mol. Biol. Cell *11*, 635–645.

Slot, J. W., and Geuze, H. J. (2007). Cryosectioning and immunolabeling. Nat. Protoc. *2*, 2480–2491.

Stephens, D. J., Lin-Marq, N., Pagano, A., Pepperkok, R., and Paccaud, J. P. (2000). COPI-coated ER-to-Golgi transport complexes segregate from COPII in close proximity to ER exit sites. J. Cell Sci. *113*, 2177–2185.

Ward, T. H., Polishchuk, R. S., Caplan, S., Hirschberg, K., and Lippincott-Schwartz, J. (2001). Maintenance of Golgi structure and function depends on the integrity of ER export. J. Cell Biol. *155*, 557–570.

Waters, M. G., and Blobel, G. (1986). Secretory protein translocation in a yeast cell-free system can occur posttranslationally and requires ATP hydrolysis. J. Cell Biol. *102*, 1543–1550.

Weibel, E. R. and Bolender, R. P. (1979) Stereological Methods, London, United Kingdom: Academic Press.

Whyte, J.R.C., and Munro, S. (2002). Vesicle tethering complexes in membrane traffic. J. Cell Sci. *115*, 2627–2637.

Wilson, B. S., Nuoffer, C., Meinkoth, J. L., McCaffery, M., Feramisco, J. R., Balch, W. E., and Farquhar, M. G. (1994). A Rab1 mutant affecting guanine nucleotide exchange promotes disassembly of the Golgi apparatus. J. Cell Biol. *125*, 557–571.

Wu, W. J., Erickson, J. W., Lin, R., and Cerione, R. A. (2000). The gamma-subunit of the coatomer complex binds Cdc42 to mediate transformation. Nature *405*, 800–804.

Xu, D., and Hay, J. C. (2004). Reconstitution of COPII vesicle fusion to generate a pre-Golgi intermediate compartment. J. Cell Biol. *167*, 997–1003.

Yu, S., Satoh, A., Pypaert, M., Mullen, K., Hay, J. C., and Ferro-Novick, S. (2006). mBet3p is required for homotypic COPII vesicle tethering in mammalian cells. J. Cell Biol. *174*, 359–368.